RESEARCH

3T-MRI-based age, sex and site-specific markers of musculoskeletal health in healthy children and young adults

Huda M Elsharkasi[1], Suet C Chen[1], Lewis Steell[1], Shuko Joseph[1,2], Naiemh Abdalrahaman[1], Christie McComb[3], Blair Johnston[3], John Foster[3], Sze Choong Wong[1] and **S Faisal Ahmed[1]**

[1]Developmental Endocrinology Research Group, University of Glasgow, Glasgow, UK
[2]Paediatric Neurosciences Research Group, Royal Hospital for Children, NHS Greater Glasgow & Clyde, Glasgow, UK
[3]Department of Clinical Physics, NHS Greater Glasgow & Clyde, Glasgow, UK

Correspondence should be addressed to S F Ahmed: faisal.ahmed@glasgow.ac.uk

Abstract

Objective: The aim of this study is to investigate the role of 3T-MRI in assessing musculoskeletal health in children and young people.
Design: Bone, muscle and bone marrow imaging was performed in 161 healthy participants with a median age of 15.0 years (range, 8.0, 30.0).
Methods: Detailed assessment of bone microarchitecture (constructive interference in the steady state (CISS) sequence, voxel size 0.2 × 0.2 × 0.4 mm^3), bone geometry (T1-weighted turbo spin echo (TSE) sequence, voxel size 0.4 × 0.4 × 2 mm^3) and bone marrow (^{1}H-MRS, point resolved spectroscopy sequence (PRESS) (single voxel size 20 × 20 × 20 mm^3) size and muscle adiposity (Dixon, voxel size 1.1 × 1.1 × 2 mm^3).
Results: There was an inverse association of apparent bone volume/total volume (appBV/TV) with age ($r = -0.5$, $P < 0.0005$). Cortical area, endosteal and periosteal circumferences and muscle cross-sectional area showed a positive association to age ($r > 0.49$, $P < 0.0001$). In those over 17 years of age, these parameters were also higher in males than females ($P < 0.05$). This sex difference was also evident for appBV/TV and bone marrow adiposity (BMA) in the older participants ($P < 0.05$). AppBV/TV showed a negative correlation with BMA ($r = -0.22$, $P = 0.01$) which also showed an association with muscle adiposity ($r = 0.24$, $P = 0.04$). Cortical geometric parameters were highly correlated with muscle area ($r > 0.57$, $P < 0.01$).
Conclusions: In addition to providing deep insight into the normal relationships between bone, fat and muscle in young people, these novel data emphasize the role of MRI as a non-invasive method for performing a comprehensive and integrated assessment of musculoskeletal health in the growing skeleton.

Key Words
- adiposity
- bone
- marrow
- muscle
- MRI

Endocrine Connections (2022) **11**, **e220034**

Introduction

Areal bone mineral density (BMD), as assessed by dual energy X-ray absorptiometry (DXA), has been widely used as the gold standard for diagnosing osteoporosis and identifying skeletal fragility (1). However, the majority of fragility fractures occur in individuals who do not have low BMD (2) and it is possible that the poor sensitivity of DXA can be attributed to its inability to capture all aspects of bone structure and quality that influence bone strength. The link between BMD and skeletal fragility is particularly tenuous in young people where the pathophysiology of skeletal fragility may be attributed to a wide range of abnormalities in osteoblast and osteoclast activity (3, 4).

https://ec.bioscientifica.com
https://doi.org/10.1530/EC-22-0034

In addition to osteoblasts, mesenchymal stem cells are also the precursor of marrow adipocytes, and the differentiation of these stem cells to these two cell lineages is competitive and reciprocally regulated (5). Bone marrow adiposity (BMA) itself is increasingly recognised to have a strong link to bone health, and an assessment of BMA may be able to provide indirect information on osteoblast activity (6). Secondary osteoporosis is also encountered in people with reduced mobility and muscle deficits such as muscular dystrophies (7). Thus, an improved understanding of this wider range of skeletal determinants of osteoporosis has led to a greater interest in alternative methods of imaging. MRI can provide detailed information on bone structure and microarchitecture (8) to such an extent that it has often referred to as a 'virtual biopsy' (9). Furthermore, when combined with MR spectroscopy, it can be an ideal modality for quantifying compartments such as muscle and bone marrow, as well as adiposity within these organs (10). It can be performed on repeated occasions with good correlation to bone histomorphometry and micro CT (11) and vertebral BMA (12). Preliminary studies have also raised the potential of a combined assessment of microarchitecture and marrow adiposity for differentiating between different aetiologies of osteoporosis (13). The use of MRI to perform a combined evaluation of bone microarchitecture and BMA in children has rarely been reported (14). Furthermore, while there are reports of age- and sex-related changes in bone microarchitecture (15) and BMA (16, 17, 18) in healthy children and adults, there is a scarcity of knowledge on the normal relationships between these parameters (19, 20).

The current study was performed to improve our knowledge of the normal changes in the developing skeleton, as assessed by MRI, as well as to compare the bone microarchitecture information obtained from the tibia and the femur. It is anticipated that a greater understanding of normal MRI-based changes will facilitate the application of these techniques for studying the developing skeleton in more detail in health and disease.

Methods

The study cohort

A total of 161 healthy male (n = 76) and female (n = 85) children and young people with a median age of 15 years (8, 30) were recruited from families and friends of patients and staff at hospitals in Glasgow, UK. The median age of males and females was 13.8 years (8.0, 29.1) and 18.0 years (8.4, 30.0), respectively ($P < 0.006$). None of the participants had a chronic illness requiring therapy or were on any medications that are known to affect bone metabolism. In addition to anthropometric data, information was collected on current medications, use of nutritional supplements, fracture history, use of oral contraceptives and physical activity. Among the male participants, three had asthma and used glucocorticoid inhaler, and one had eczema that did not require any glucocorticoid therapy. Among the female participants, three had asthma and were on inhaler salbutamol, three were taking oral contraceptives and one had been receiving nifedipine for 3 months. One female participant had polycystic ovarian syndrome but was not receiving any medication and three female participants were smokers. The males and females had similar levels of physical activity and use of vitamin supplements. Sixteen males and 15 females had a history of traumatic fracture. The study was approved by the West of Scotland NHS Research Ethics Committee, and all participants and/or their parents/guardians provided written informed consent.

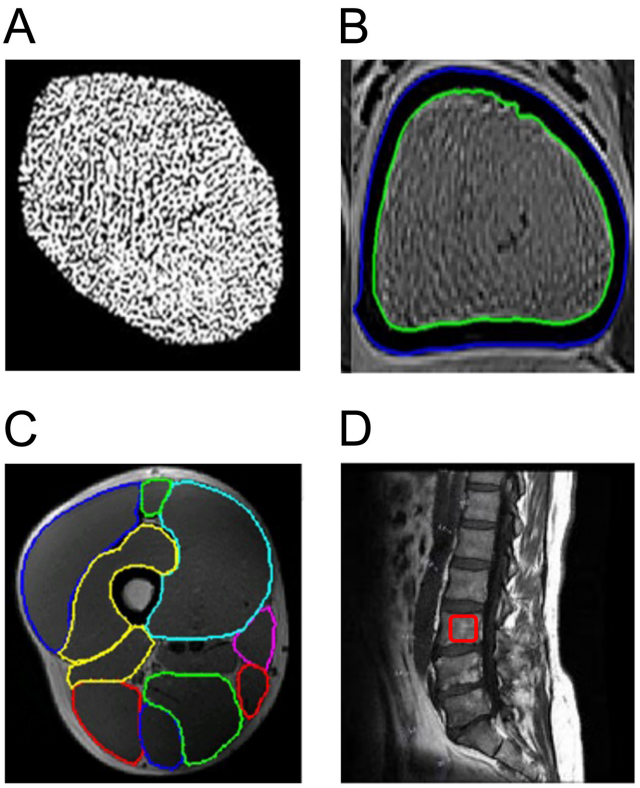

Figure 1
Representative MRI and MRS analysis images. (A) Trabecular analysis; (B) cortical analysis, green and blue lines indicate endosteal and periosteal circumferences, respectively; (C) muscle analysis, ten manually drawn regions of interest around midthigh muscles; (D) MR image of the lumbar spine with the MRS voxel location (marked with a red square) placed in L3.

Assessment of microarchitecture

MRI for trabecular microarchitecture was performed on a 3T-MRI scanner (Prisma, Siemens) at either the right tibia or femur (Fig. 1). At the tibia, images were acquired using a transmit/receive extremity coil placed over the right knee. The first slice was positioned just immediately distal to the proximal growth plate, and the subsequent slices positioned distal along the tibia. At the femur, an 18-channel anterior array coil was used to scan at 15% of distal femoral length which was measured using localizer images as the total distance between superior aspect of femoral head to the distal aspect of medial condyle. The location of 15% was chosen so that cortical geometry and trabecular microarchitecture could both be assessed in the femur in a single scan. Imaging was performed using a constructive interference in the steady state (CISS) pulse sequence with the following parameters to provide a 3D volume of a resolution = 0.2 mm × 0.2 mm × 0.4 mm echo time = 5.68 ms, repetition time = 12.62 ms, flip angle = 50°, no. of averages = 4, field of view = 100 mm × 100 mm, matrix = 448 × 448, number of slices = 20, bandwidth (Hz) = 228 and total scan time = 9:24 min. The images were analysed by MATLAB software (Mathworks Inc), to obtain measurements for apparent bone volume to total volume ratio (appBV/TV), apparent trabecular number (appTbN), apparent trabecular thickness (appTbTh) and apparent trabecular separation (appTbSp) (21). To increase contrast along edges, a sharpening filter using 'imsharpen', a MATLAB function, was applied to trabecular images. Additionally, a low pass filter was applied to the images to correct for any bone marrow inhomogeneity and a visual qualitative assessment for participant motion and image artefacts was also performed by two observers. The analysis was performed to obtain trabecular measures from the central slice (slice 10) from 20 slices per participant. Mean intraobserver and interobserver coefficient of variations were both ~1% for the trabecular parameters measured.

Cortical imaging

For analysis of cortical bone at the right femur, 20 axial images were obtained at 15% of distal femoral length with a central slice co-located with the central slice of trabecular bone images (Fig. 1). The T1-weighted turbo spin echo (TSE) pulse sequence with parallel imaging (GRAPPA acceleration factor PE: 2) was used with the following acquisition voxel size = 0.4 mm × 0.4 mm × 2 mm, echo time = 11 ms, repetition time = 650 ms, flip angle = 150°, no. of averages = 1, field of view = 140 mm × 140 mm, matrix = 320 × 240, number of slices = 20, bandwidth (Hz) = 240 and total scan time = 1:05 min. The images were analysed using MATLAB (Mathworks Inc) to obtain measurements for cortical area (mm^2) and endosteal and periosteal circumferences (mm). A sharpening filter was applied to increase contrast between edges as mentioned above. Mean intraobserver and interobserver coefficient of variations were 2 and 1% for the cortical parameters, respectively.

Muscle imaging

Axial images were obtained at 33% of distal femoral length to examine ten groups of thigh muscles (Fig. 1). A six-point Vibe Dixon pulse sequence in 3D with parallel imaging (GRAPPA acceleration factor PE: 2) was used with the following acquisition parameters: voxel size= 1.1 mm × 1.1 mm × 2 mm, echo time = 1.54–8.69 ms (TE1 = 1.54 ms, deltaTE = 1.43 ms), repetition time = 10.7 ms, flip angle = 4°, no. of averages = 6, field of view = 204 mm × 204 mm, number of slices = 20 and bandwidth (Hz/Px) = 434. Bipolar readout was used with a total scan time = 3.00 min. The images were then analysed to obtain measurements of muscle fat fraction as a percentage (MFF%), total muscle cross-sectional area (muscle CSA, mm^2) and residual muscle area (i.e. muscle tissue after accounting for muscle fat fraction (RMA, mm^2) (22). Mean intraobserver and interobserver coefficient of variations were 1.7 and 1%, respectively.

Bone marrow adiposity

^{1}H-MRS was performed using an 18-channel body array (anterior) and a 32-channel spine coil (posterior). Spectra were obtained from a 20 mm × 20 mm × 20 mm volume within the vertebral body of L3, using a method described previously (13). A point resolved spectroscopy sequence (PRESS) with no water suppression was used with the following parameters: echo time = 30 ms, repetition time = 2000 ms, flip angle = 90°, no. of averages = 80, bandwidth (Hz) = 1200 and total scan time = 2:50 min. Automated phase cycling was performed with four preparation scans and one reference scan. Analysis was performed following fitting of the spectrum in the time domain using a non-linear least-squares algorithm, AMARES (23) in the java-based MR user interface (JMRUI) software package (24). The areas under the water peak and lipid peak were obtained and used to calculate the lipid-to-water ratio (LWR) and percentage bone marrow fat fraction (BMFF%) as a measure of BMA (25). Mean intraobserver and interobserver coefficient of variations were both 2.5%.

https://ec.bioscientifica.com
https://doi.org/10.1530/EC-22-0034

Statistical analyses

All data were analysed using IBM SPSS for Windows software program, Version 22 and GraphPad Prism 8.0.2 (GraphPad Software). Continuous data were presented as median (ranges) and categorical data as frequency (percentage). Group differences were compared by a Mann–Whitney *U* test for continuous variables and a chi-square test for categorical variables. Sex differences in MRI-based parameters were assessed using Mann–Whitney *U* tests. Sex differences were tested using analysis of covariance with age as a covariate. Spearman's rank correlations and multiple regression analyses were performed to investigate associations between musculoskeletal outcomes and age, sex and anthropometric variables in the whole cohort and in males and females separately. A P value of <0.05 was considered significant. Residual plots for all models were checked for normality, linearity and homoscedasticity. Due to a potential multicollinearity between predictor variables, any variable with a variance inflation factor (VIF) 10 and tolerance value <0.2 was excluded from the models.

Results

Trabecular bone microarchitecture at tibia and femur

Of the 161 participants who had scans, 138 (86%) had an assessment of trabecular microarchitecture and, of these, the scans were of sufficient quality to be analysed in 128 (93%). Of these 128, a tibia scan was performed in 55 (44%) (M:F, 29:26), with a median age of 13.4 years (8.1, 18.9) and a femur scan was performed in 73 (57%) (M:F, 42:31) with a median age of 15.0 years (8.0, 29.1) (P=0.006). There were no differences between sexes in any of the trabecular parameters in the tibia or femur at any ages, except in the age group >18 years where appBV/TV was marginally but significantly higher in males (Fig. 2 and Table 1). An age-dependent decline was observed in appBV/TV in males and females at the tibia and femur (Fig. 3). Conversely, appTbSp increased with age and was accompanied by a significant decrease in appTbN (Fig. 3). Comparing the trabecular parameters in all those with a tibia scan to those with a femur scan, median appBV/TV was 0.59 (0.53, 0.64) and 0.55 (0.50, 0.61), appTbN was 2.00 (1.79, 2.20) and 1.85 (1.59, 2.08) and appTbSp was 0.20 (0.17, 0.26) and 0.24 (0.20, 0.29) (P<0.0001), respectively (Fig. 4). Trabecular thickness showed no age, sex or site dependency (Fig. 4 and Table 1). Age was a significant predictor of trabecular microarchitecture at proximal tibia when controlling for height and BMI and explained 33–45% of variations in trabecular microarchitecture.

Cortical bone geometry at femur

Of the 161 participants, 80 (50%) had a femur scan for collecting cortical bone geometry and in 79 (99%), the cortical images were of sufficient quality to be analysed. The median age of this cohort of 79 (M:F, 46:33) participants was 15.5 years (8.0, 29.1). Sex-specific differences were only observed in periosteal circumference and cortical area in the older age group (Fig. 2), but along with endosteal circumference, both parameters showed an age-dependent increase in both sexes (Fig. 3). Cortical area, periosteal and endosteal circumferences adjusted for age showed that males had higher values than females; for cortical area, a sex difference was only evident in the older age groups (Table 2). Similarly, for periosteal and endosteal circumferences, differences were evident within the 17–19 age group (P<0.001) (Fig. 2 and Table 2). In a multiple linear regression model that included age, sex, height, BMI and muscle CSA, height, muscle CSA and age were the main predictors for cortical area and that model explained 68% of variation with age (Table 3). Height was the main predictor for endosteal (β=0.78 P=0.001) and periosteal circumferences (β=0.82 P=0.001) when age, sex, BMI and muscle CSA were controlled (Table 3).

Muscle imaging at femur

Of the 80 participants who had a femur scan, the muscle images were of sufficient quality to be analysed in 78 (98%) (M:F, 44:34) and the median age was 15.0 years (8.0, 29.1). For muscle CSA, a clear difference between males and females was evident in the late teenage years (Fig. 2 and Table 2). However, this sex- dependency was not evident for MFF% and, as a consequence, the RMA also showed the same sex dependency as muscle CSA (Fig. 2). While muscle CSA and RMA also showed a clear increase with age, MFF did not show this increase (Fig. 2). Adjusted muscle CSA and RMA for age showed males had higher values than females; for muscle CSA, this gender difference appeared within the 17–19 age group (P=0.001) and the 20–30 age group (P=0.0003). Similarly, for RMA, differences were evident within the 17–19 age group (P=0.008) and the 20–30 age group (P=0.0004). On multiple regression analysis, age, sex, BMI and height had independent associations with muscle CSA and explained 76% of the variation (Table 3). On the other hand, BMI was the main predictor (β=0.09 P=0.01) for MFF% when age and weight were controlled (Table 3).

https://ec.bioscientifica.com
https://doi.org/10.1530/EC-22-0034

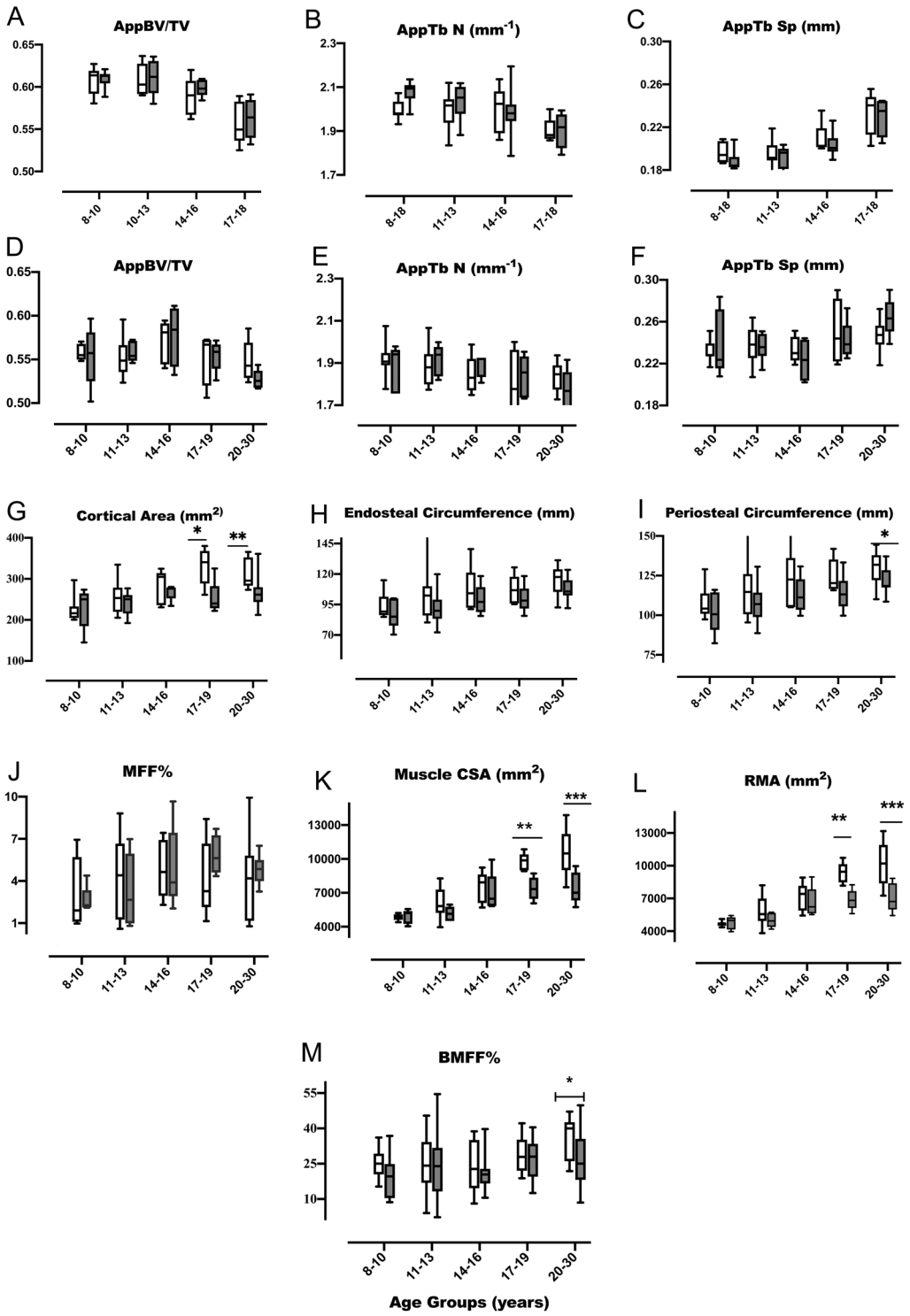

Figure 2

MRI-based musculoskeletal parameters for age and sex. Boxplots show the normative data of the MRI-based parameters and demonstrate the association of sex (white boxes for males and the grey for females) and age with these parameters. A significant sex difference within an age group is identified by $^{*}P < 0.05$. $^{**}P < 0.01$, $^{***}P < 0.001$ Panels (A, B and C) show trabecular microarchitecture at proximal tibia, panels (D, E amd F) show trabecular microarchitecture at distal femur, panels (G to I) show cortical geometry parameters at femur, panels (J, K and L) show skeletal muscle parameters at femur and panel (M) shows marrow adiposity at lumbar vertebrae. AppBV/TV, apparent bone volume over total volume; appTbTh, apparent trabecular thickness; appTb N, apparent trabecular number; appTb Sp, apparent trabecular separation; MFF, mean fat fraction (muscle); muscle CSA, muscle cross-sectional area; RMA, residual muscle area; BMFF, bone marrow fat fraction.

https://ec.bioscientifica.com
https://doi.org/10.1530/EC-22-0034

Table 1 MRI-based parameters of trabecular microarchitecture across age groups in healthy young volunteers.

	Males						Females					
Age (years)	8–10	11–13	14–16	17–18	19–30	Whole cohort	8–10	11–13	14–16	17–18	19–30	Whole cohort
Tibia (n = 55)	7	12	5	5		29	6	8	8	4		26
AppBV/TV	0.614 (0.580, 0.623)	0.603 (0.590, 0.637)	0.590 (0.562, 0.620)	0.549 (0.525, 0.589)	–	0.594 (0.525, 0.637)	0.613 (0.588, 0.621)	0.612 (0.580, 0.635)	0.598 (0.584, 0.609)	0.563 (0.532, 0.591)	–	0.605 (0.532, 0.636)
AppTb Th (mm)	0.300 (0.289, 0325)	0.308 (0.280, 0.326)	0.294 (0.268, 0.320)	0.294 (0.283, 0.304)	–	0.300 (0.268, 0.326)	0.294 (0.285, 0.297)	0.299 (0.280, 0.328)	0.303 (0.266, 0.334)	0.295 (0.278, 0.314)	–	0.2974 (0.266, 0.334)
AppTb N (mm^{-1})	1.980 (1.931, 2.073)	2.016 (1.835, 2.120)	2.024 (1.860, 2.136)	1.882 (1.858, 2.000)	–	2.006 (1.858, 2.136)	2.094 (1.977, 2.135)	2.052 (1.882, 2.118)	1.981 (1.787, 2.195)	1.917 (1.792, 1.994)	–	2.005 (1.787, 2.195)
AppTb Sp (mm)	0.194 (0.186, 0.209)	0.191 (0.179, 0.203)	0.203 (0.200, 0.236)	0.240 (0.203, 0.256)	–	0.203 (0.179, 0.256)	0.184 (0.182, 0.208)	0.196 (0.172, 0.204)	0.200 (0.189, 0.226)	0.235 (0.205, 0.245)	–	0.199 (0.172, 0.245)
Femur (n = 73)	7	14	5	4	12	42	5	6	4	6	11	31
AppBV/TV	0.554 (0.548, 0.571)	0.549 (0.523, 0.596)	0.581 (0.540, 0.595)	0.567 (0.506, 0.573)	0.542* (0.524, 0.585)	0.551 (0.506, 0.596)	0.557 (0.502, 0.597)	0.554 (0.549, 0.572)	0.584 (0.532, 0.611)	0.559 (0.526, 0.572)	0.525* (0.517, 0.544)	0.550 (0.502, 0.611)
AppTb Th (mm)	0.294 (0.265, 0.312)	0.294 (0.260, 0.322)	0.321 (0.276, 0.332)	0.303 (0.281, 0.344)	0.295 (0.272, 0.329)	0.295 (0.260, 0.344)	0.290 (0.282, 0.316)	0.294 (0.284, 0.334)	0.313 (0.278, 0.318)	0.297 (0.287, 0.327)	0.297 (0.283, 0.311)	0.299 (0.278, 0.372)
AppTb N (mm^{-1})	1.907 (1.777, 2.075)	1.879 (1.773, 2.066)	1.830 (1.748, 1.987)	1.777 (1.663, 2.000)	1.847 (1.728, 1.937)	1.855 (1.663, 2.075)	1.941 (1.755, 1.979)	1.939 (1.820, 1.999)	1.919 (1.806, 1.925)	1.855 (1.732, 1.953)	1.768 (1.591, 1.952)	1.849 (1.591, 1.999)
AppTb Sp (mm)	0.228 (0.217, 0.251)	0.238 (0.207, 0.264)	0.230 (0.219, 0.290)	2.444 (0.219, 0.290)	0.247* (0.219, 0.272)	0.239 (0.207, 0.290)	0.224 (0.208, 0.284)	0.235 (0.214, 0.251)	0.223 (0.202, 0.244)	0.238 (0.225, 0.273)	0.263* (0.239, 0.290)	0.242 (0.202, 0.290)

The significance of a sex difference within an age group is indicated by the superscript: $^{*}P < 0.05$.

AppBV/TV, apparent bone volume over total volume; appTb N, apparent trabecular number; appTb Sp, apparent trabecular separation; appTbTh, apparent trabecular thickness; endos circ, endosteal circumference; perios circ, periosteal circumference.

https://ec.bioscientifica.com
https://doi.org/10.1530/EC-22-0034

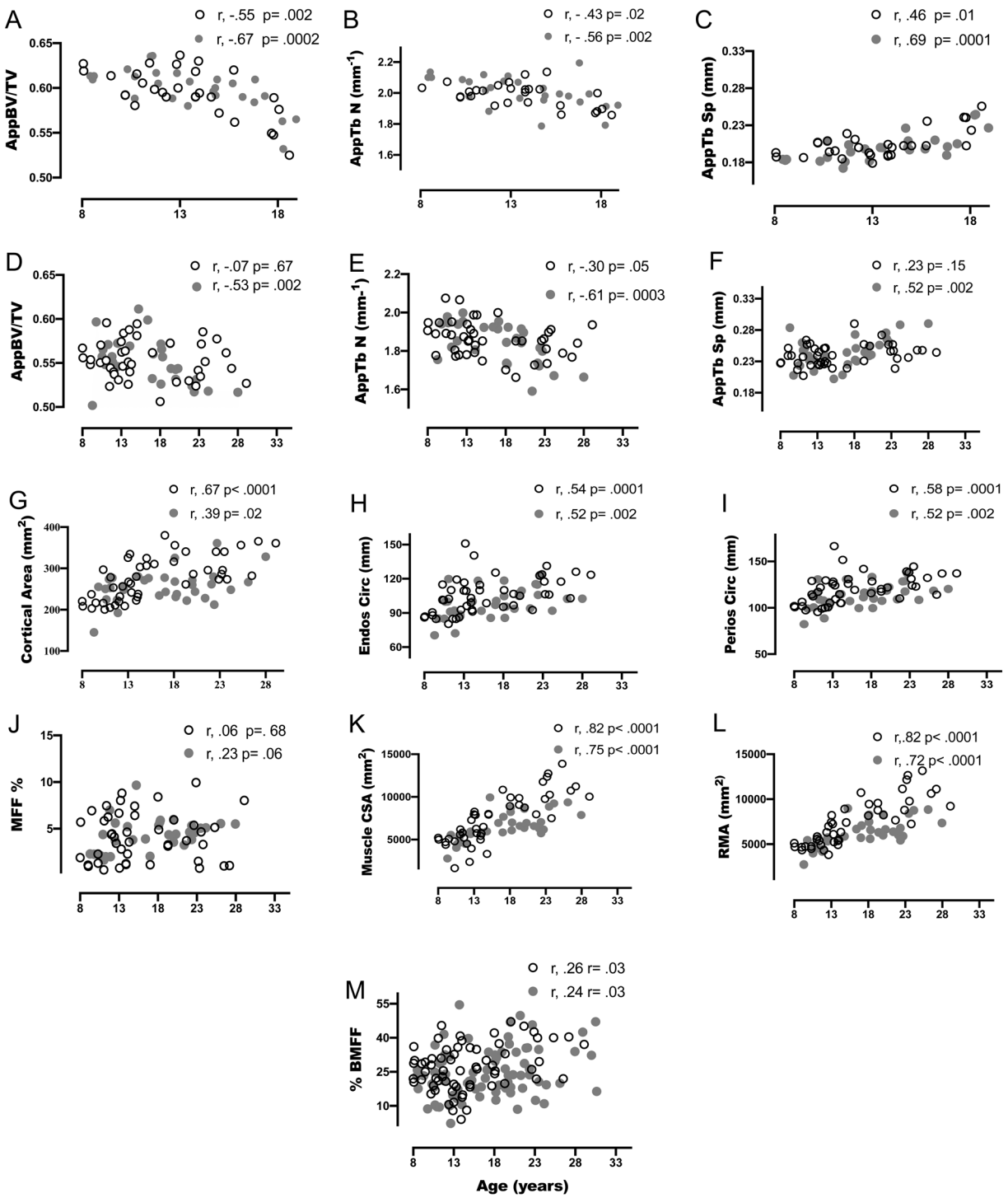

Figure 3

Association between MRI-based musculoskeletal parameters and age. The scatter plots show MRI-based measures in males (white circles) and females (grey circles). Panels (A, B and C) show trabecular microarchitecture at proximal tibia, panels (D, E and F) show trabecular microarchitecture at distal femur, panels (G to I) show cortical geometry parameters at femur, panels (J, K and L) show skeletal muscle parameters at femur and panel (M) shows marrow adiposity at lumbar vertebrae. AppBV/TV, apparent bone volume over total volume; appTbTh, apparent trabecular thickness; appTb N, apparent trabecular number; appTb Sp, apparent trabecular separation; endos circ, endosteal circumference; perios circ, periosteal circumference; MFF, mean fat fraction (muscle); muscle CSA, muscle cross-sectional area; RMA, residual muscle area; BMFF, bone marrow fat fraction.

https://ec.bioscientifica.com
https://doi.org/10.1530/EC-22-0034

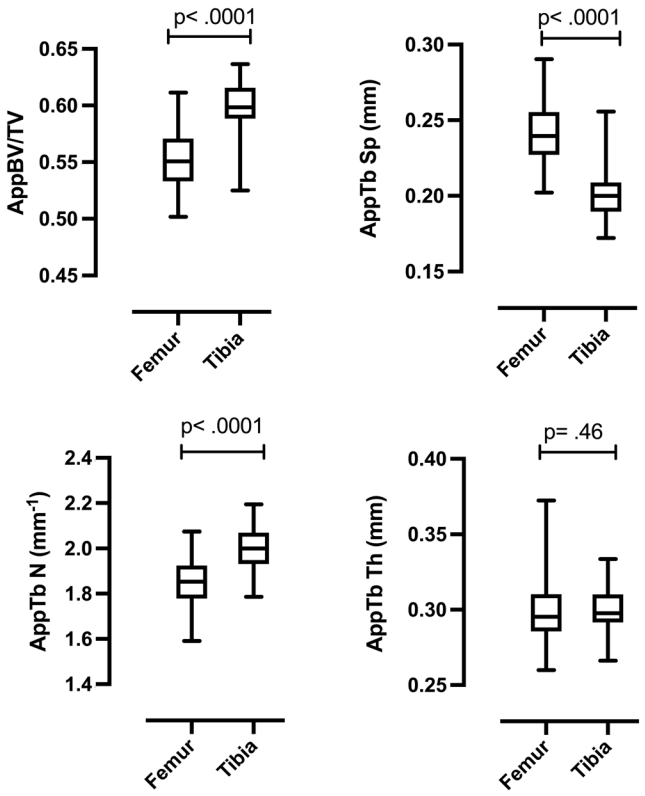

Figure 4
MRI-trabecular microarchitecture in tibia vs femur. AppBV/TV, apparent bone volume over total volume; appTbTh, apparent trabecular thickness; appTb N, apparent trabecular number; appTb Sp, apparent trabecular separation.

Bone marrow adiposity at spine

All 161 participants had MRS and the images were of sufficient quality to be analysed in 143 (89%) (M:F, 65:78) in whom the median age was 15.0 years (8.0, 30.0). For BMA as expressed by BMFF%, a clear difference between sexes was only seen in young adulthood when it was higher in males compared to females (Fig. 2 and Table 1). BMFF% also showed an increase with age, but this association was not as strong as it was for the other markers of musculoskeletal health. Adjusted BMFF% for age showed higher values in males than females ($P=0.04$). On multiple regression analysis, the model showed that age and sex had independent associations with BMFF%, but they still only accounted for only 9.4% of the latter.

Intercompartmental relationships

In the 73 participants who had analysable trabecular and cortical femur data, no association was observed between any trabecular parameters with cortical or muscle parameters (Table 4). An inverse association was observed between appBV/TV of tibia and femur ($r=0.22$, $P=0.01$) with BMFF% in the 111 participants where these data were available (Table 4). Cortical geometrical measures showed a positive association to BMFF%, but these associations did not persist after adjusting for age and height (Table 5). Positive associations were also observed between the cortical measures and muscle CSA (Table 5), and the association between cortical area and muscle CSA persisted even after height adjustment ($\beta = 0.30$ $P=0.02$) (Table 5), while the association with endosteal and periosteal circumference did not persist ($P>0.05$). BMFF% showed a weak but significant association with muscle adiposity as measured by MFF% ($r=0.24$, $P=0.04$) (Table 5).

Discussion

The current study represents the largest report of the use of 3T-MRI for the assessment of multiple musculoskeletal parameters in healthy males and females from late childhood, through adolescence and into young adulthood. In over 90% of cases, the scans that were performed were suitable for analysis confirming the suitability of MRI at the young age group. It was also reassuring to observe that the intercompartmental relationships that have been observed through other imaging modalities continue to be present on using MRI.

The assessment of trabecular bone microarchitecture at two major weight-bearing sites showed a progressive decrease in trabecular bone architecture in both sexes, especially at the proximal tibia. This decline in trabecular parameters has been described previously in young adults at the distal radius, tibia and lumbar spine (26, 27). This pattern has also been observed in children at the proximal femur using μCT falling to expected values in adults (28, 29). In fact, it is possible that trabecular bone volume fraction at the proximal tibia may be highest at birth, decreasing towards the adult pattern as early as 8 years of age (30). The biological explanation for the tibial finding may be a decreased sensitivity of trabecular bone to oestrogen (26). In addition, trabecular bone development may be less dependent on the growth hormone/insulin-like growth factor 1 axis, unlike cortical bone mass (31). In fact, high growth hormone levels as encountered during puberty could actually be an explanation for the reduction in trabecular bone that may be associated with high bone turnover (26, 32). The differences in observations at the tibial and femoral site may reflect the varying level of corticalization of the trabeculae at the regions of interest and emphasize the importance of site specificity when

Table 2 MRI-based parameters of musculoskeletal health across age groups in healthy young volunteers.

	Males						Females					
	8–10	11–13	14–16	17–19	20–30	Whole cohort	8–10	11–13	14–16	17–19	20–30	Whole cohort
Cortical (n = 79)	8	15	6	5	12	46	5	6	5	6	11	33
Cortical area (mm^2)	216 (200, 297)	253.4 (205, 335)	305 (231, 324)	341** (261, 380)	296*** (273, 361)	276 (200.4, 380.1)	250 (145, 274)	251 (192, 277)	276 (234, 280)	240** (222, 325)	262*** (212, 361)	255 (145.1, 361)
Endosteal circumference (mm)	89.3 (84.8, 114.9)	102.4 (80.4, 151)	104.2 (91.3, 140.5)	106.7 (95.3, 125.5)	117.6 (92.6, 131.3)	104.1 (80.4, 151)	85.1 (70.4, 100.0)	89.9 (72.2, 119.8)	97.1 (85.7, 118.3)	98.2 (85.7, 118.3)	105.8 (91.9, 123.5)	99.95 (70.4, 123.5)
Periosteal circumference (mm)	104.2 (97.4, 129.0)	114.7 (95.5, 166.5)	122.5 (105.1, 151.7)	120.3 (115.7, 141.9)	131.8*** (110, 144.5)	119.8 (95.5, 166.5)	100.6 (82.32, 116.1)	107 (88.67, 130.6)	111.2 (99.7, 130.8)	113.1 (99.7,133.3)	118.5*** (108.6, 137.1)	112.7 (82.3, 137.1)
Muscles (n = 78)	7	15	5	5	12	44	5	6	5	6	12	34
MFF%	1.9 (0.97, 6.93)	4.4 (0.59, 8.81)	4.64 (2.30, 7.43)	3.28 (1.14, 8.41)	4.19 (2, 9.94)	3.9 (0.6, 9.9)	2.30 (2.10, 4.38)	2.67 (0.80, 6.98)	3.90 (2.04, 9.66)	5.63 (4.35, 7.70)	4.85 (3.25, 6.51)	4.5 (0.8, 9.7)
Muscle CSA (mm^2)	4802 (4394, 5214)	5829 (3957, 8269)	7922 (5699, 9240)	9872** (8923, 10,847)	10,496*** (7501, 13,881)	7692 (3957, 13,881)	5207 (4038, 5555)	5145 (4502, 5952)	6475 (5830, 9936)	7339** (6070, 8714)	7004*** (5734, 9363)	6338 (4038, 9936)
RMA (mm^2)	4706 (4351, 5115)	5559 (3821, 8205)	7410 (5434, 8909)	9452** (8172, 10,723)	10,203*** (7252, 13,168)	7252 (3821, 13,168)	4978 (3952, 5429)	4948 (4188, 5733)	6229 (5525, 8976)	6830** (5602, 8247)	6715*** (5428, 8843)	6001 (3952, 8976)
BMA (n = 143)	26	35	20	25	37	65	15	20	10	9	11	78
BMFF%	22.6 (8.7, 36.8)	24.0 (2.3, 54.6)	20.4 (8.1, 39.7)	27.9 (12.6, 42.2)	29.0* (8.5, 49.8)	26.2 (4 .0, 47.1)	25.1 (15.3, 36.1)	24.2 (4.0, 45.4)	22.8 (8.1, 38.7)	27.9 (18.8, 42.2)	40.0* (21.9, 47.13)	23.5 (2.3, 54.6)

The significance of a sex difference within an age group is indicated by the superscript: *$P < 0.05$; **$P < 0.01$; ***$P < 0.\ 001$.
BMA, bone marrow adiposity; BMFF, bone marrow fat fraction; MFF%, percentage of total muscle fat fraction; Muscle CSA, muscle cross-sectional area; RMA, remaining muscle area.

https://ec.bioscientifica.com
https://doi.org/10.1530/EC-22-0034

Table 3 Predictors of MRI-based musculoskeletal measures in multiple regression analysis. Models for trabecular microarchitecture included age, height and BMI as predictors. The cortical geometry models included age, sex, height, BMI and muscle CSA as predictors. Model for MFF included age, weight and BMI, whereas models for other muscle parameters included age, sex, height and BMI. BMA model included age, sex and BMI. Statistically significant was set at $P < 0.05$.

	Significant predictors	Unstandardized coefficient		Standardized coefficient	*P* value	Adjusted R^2	Collinearity statistics	
		B	S.E.	β			Tolerance	VIF
Trabecular microarchitecture (tibia)								
AppBV/TV	Age	−0.006	0.001	−0.79	0.000	40%	0.36	2.7
AppTb N (mm^{-1})	Age	−0.01	0.006	−0.49	0.02	33%	0.35	2.9
AppTb Sp (mm)	Age	0.004	0.001	0.68	0.001	45%	0.39	2.6
Cortical geometry (femur)								
Cortical area	Height	2.53	0.45	0.72	0.000	68%	0. 29	3.35
	Muscle CSA	0.01	0.003	0.47	0.003		0.45	2.24
	Age	−2.62	1.12	−0.30	0.02		0.69	1.43
Endosteal circumference (mm)	Height	0.86	0.18	0.78	0.000	48%	0.30	3.29
Periosteal circumference (mm)	Height	0.90	0.17	0.82	0.000	52%	0.31	3.29
Muscles (femur)								
MFF%	Age	0.50	0.14	0.09	0.01	28%	0.37	2.68
Muscle CSA (mm^2)	Age	124	39	0.30	0.002	76%	0.35	2.8
	Height	50	15	0.33	0.001		0.35	2.8
	BMI	184	38	0.34	0.000		0.62	1.6
	Sex	−1216	273	−0.27	0.000		0.88	1.1
RMA (mm^2)	Age	125	40	0.32	0.003	74%	0.35	2.9
	Height	50	15	0.34	0.001		0.35	2.9
	BMI	147	39	0.29	0.000		0.62	1.6
	Sex	−1186	278	−4.3	0.000		0.88	1.1
BMA (vertebra)								
BMFF%	Age	0.41	0.19	0.22	0.03	9.4%	0.67	1.49
	Sex	−3.5	1.74	−0.17	0.04		0.95	1.1

AppBV/TV, apparent bone volume over total volume; appTb N, apparent trabecular number; appTb Sp, apparent trabecular separation; appTbTh, apparent trabecular thickness; BMFF, bone marrow fat fraction; MFF, mean fat fraction; Muscle CSA, muscle cross-sectional area; RMA, remaining muscle area; SE, standard error; VIF, variation inflation factor.

using high-resolution MRI. Androgens are known to play a role in the normal development of trabecular bone (33). Previous studies that have explored sex-specific differences in bone microarchitecture have revealed mixed results, but the general pattern of results suggests that these differences which report increased trabecular bone in males are more likely to be present at a later stage of puberty and may be more evident at sites that are load-bearing (15, 34, 35). Histomorphometric analysis at the iliac crest has reported the existence of sex-specific differences in trabecular microarchitecture in late puberty (36). In the current study, significant differences were only evident in the 20–30 years age group, at the distal femur, where young men showed a greater appBV/TV than women. The current study also showed that app BV/TV and app Tb.N were higher in the proximal tibia than the distal femur. It is possible that this may reflect the younger age group of those who had a tibia scan compared to those who had a femur scan. Trabecular bone microarchitecture may also vary depending on scan location with higher quality trabeculae at the epiphysis and metaphysis compared to at diaphysis (37). This finding underscores the importance of scan location and how they can have a significant influence on trabecular measurements (38). None of the parameters of bone microarchitecture showed any independent association to anthropometry or muscle parameters, but, as reported previously in adults (39, 40), the inverse association of MRI trabecular microarchitecture with bone marrow adiposity was also present in children. This finding reinforces the hypothesis that skeletal fragility may have its origins in a shift in mesenchymal stem differentiation towards adipogenesis rather than osteogenesis (41).

MRI clearly demonstrates the changes in femoral bone geometry, characterized by increases in cortical area and periosteal and endosteal expansion. These were observed in both sexes, with a higher magnitude of changes at both endosteal and periosteal surfaces in males as compared to females. Additionally, consistent with the functional model of bone development, height and muscle cross-sectional area, which measured as a surrogate of muscle force, were the primary contributors for femoral cortical bone development. These findings are consistent with

https://ec.bioscientifica.com
https://doi.org/10.1530/EC-22-0034

Table 4 Associations of MRI trabecular measures with other musculoskeletal compartments. Unadjusted correlations of femoral trabecular parameters with cortical parameters (cortical area, endosteal and periosteal circumferences); muscle parameters (cross-sectional area (CSA), remaining muscle area (RMA)); and bone marrow adiposity (bone marrow fat fraction (BMFF)).

	AppBV/TV	**AppT Sp** (mm)	**AppTb N** (mm^{-1})	**AppTbTh** (mm)
Cortical (n = 73)				
Cortical area (mm^2)	0.06	0.07	−0.19	0.23
Endosteal circumference (mm)	−0.12	0.04	−0.02	−0.06
Periosteal circumference (mm)	−0.11	0.06	−0.06	−0.01
Muscle (n = 73)				
Muscle CSA (mm^2)	0.01	0.07	−0.18	0.20
RMA (mm^2)	0.05	0.06	−0.17	0.21
*BMA (n = 111)				
BMFF%	**−0.22**	**0.24**	−0.21	−0.01

Level of significance was set <0.05 and highlighted in bold.
*Refers to the association between spinal bone marrow adiposity and trabecular measures at both tibia and femur.

several previous studies of cortical geometry (34, 42, 43, 44, 45). In the current study, sex differences were only evident in those over 17 years old and may again just reflect the smaller sample size in the younger age groups. The major independent determinants of cortical area included height and muscle CSA, as observed previously with other imaging modalities (46, 47, 48). The current work did not find a significant independent association between cortical dimensions and BMA. Unlike the inverse relationship that is found between trabecular microarchitecture and BMA, there is less consensus on the relationship between BMA and cortical geometry (49).

Table 5 Intercompartment associations between MRI-based parameters. The associations between cortical measures BMFF did not persist after controlling for age and height.

	Muscle (n = 77)			**BMA** (n = 68)
	MFF (%)	Muscle CSA (mm^2)	RMA (mm^2)	BMFF (%)
Cortical area (mm^2)	0.15	**0.73***	**0.73***	**0.37**
Endosteal circumference (mm)	0.13	**0.58**	**0.57**	**0.44**
Periosteal circumference (mm)	0.15	**0.63**	**0.62**	**0.45**
BMFF%	**0.24**	0.22	0.19	1

The significant level was set <0.05 and highlighted in bold.
*Refers to the persistent associations between cortical area with muscle CSA and RMA after height adjustment ($\beta = 0.3$, $P = 0.02$) but not with endosteal and periosteal circumferences ($P > 0.05$).

Previous histologic and MRI-based studies have reported consistently that vertebral marrow fat increases steadily with age as a result of conversion from haemopoietin (red) to fatty marrow (yellow) (50). The current study confirms the presence of this association in children and young people. The average BMFF% as a measure of BMA in the subjects was approximately 24%, which is close to the values reported by MRS-based studies for healthy participants within the same age range (12, 17). The age-related increase of vertebral marrow fat was small but significant, with sex and age as predictors explaining 10% of the variations in marrow adiposity. Previous studies have reported large inter-individual variations in the normal value of marrow fat in children and adults (17, 51). The precision of the technique in the current study was high and it is possible that the previously reported variation was due to the heterogeneity of marrow conversion. Previous studies have also reported lower marrow adiposity in females before menopause compared to males with a reversal of this trend after the menopause (12, 17, 52). The current study showed that this sexual dimorphism was also present in children and became particularly evident in the older adolescents and young adults, potentially emphasizing the role of oestrogens in influencing marrow adiposity (53). The current study did not show an independent association of marrow adiposity with BMI and is possible that marrow adiposity may be more closely related to other fat depots such as visceral fat (54).

The results of the current work showed no sex-or age-specific variations in fat fractions in the thigh muscles of healthy children and young people. The median fat fraction for ten muscle groups measured in the thigh were <10%, which is similar to that reported previously in children and adults (55). The independent role of age on fat content within muscle is not fully understood and contradictory findings are reported in the literature (56, 57). In the current study, muscle fat was not associated with age. Muscle fat fraction appears to be significantly influenced by BMI. This concurs with cross-sectional (58) and longitudinal studies (59). BMI is a crude marker of general adiposity; previous MRI-based studies by our group have shown that subcutaneous adipose tissue and visceral adipose tissue demonstrate different relationships to bone marrow fat (54). Unfortunately, this could not be explored in the current study, but there is a need to study muscle adiposity further in more detail given that its utility in being an independent marker of cardiovascular risk (60). Furthermore, a high level of fatty muscle infiltration may also be associated with a high marrow fat (57) and this was also confirmed in the current study.

https://ec.bioscientifica.com
https://doi.org/10.1530/EC-22-0034

While MRI promises to be a useful modality for an integrated assessment of musculoskeletal health in young people, it is possible that some parameters such as trabecular dimensions need careful assessment. Trabecular bone maybe subject to partial volume effects that result from the resolution offered by the MRI in comparison to the trabecular dimensions. It is also possible that some of the associations between parameters were not evident due to a limitation on sample size. MRI is an expensive technique and in combination with the lack of standardized methods of assessing the parameters, this represents a limitation of this imaging modality if it is considered for general use. Given the novelty of this modality, it is encouraging to see that there is a move towards developing greater consensus in standardizing the methodology (61). In the current study, we did not perform MR spectroscopy as it would have further prolonged the scan times. Given that there may be additional value of this condition in pathological conditions that lead to metabolic changes in the muscle compartment, this may be a useful technique to explore further (61). In addition, we did not look at markers of visceral adiposity in this study and these relationships would have also been useful to explore (18).

In summary, high-resolution MRI is a powerful tool for quantitative non-invasive assessment of musculoskeletal status *in vivo*. The observations and relationships that were reported by this tool were similar to those described previously using other modalities, thus strengthening the rationale for using MRI as an integrated measure of musculoskeletal health in children, young people, as well as adults.

Declaration of interest

The authors declare that there is no conflict of interest that could be perceived as prejudicing the impartiality of the research reported.

Funding

This work did not receive any specific grant from any funding agency in the public, commercial, or not-for-profit sector.

Author contribution statement

H M E recruited the cases, performed the study, analysed the data and wrote the manuscript, N A, L S, S J and S C C recruited the cases, performed the study and revised the manuscript, C M assisted with the design of the study, devised the MRI protocol and revised the manuscript, J F and B J devised the MRI protocol and revised the manuscript, S C W assisted with the design of the study and revised the manuscript, S F A conceived and designed the study, performed the analysis, wrote the manuscript and acts as the guarantor.

Acknowledgements

The authors would like to thank Caroline Crosbie, Laura Dymock, Evonne McLennan, Rosemary Woodward for their assistance with image acquisition. N A and H M E were supported by the Libyan Ministry for Higher Education. S C C and L S were supported by the Glasgow Children's Hospital Charity Research Fund and S C C is currently supported by a N H S Research Scotland Career Researcher Fellowship. C M was supported through the Scottish Academic Health Sciences Collaboration. B J was supported by the Medical Fund of the University of Glasgow. S J was supported by a NHS Research Scotland Chief Scientist Office Clinical Academic Fellowship.

References

1 NIH Consensus Development Panel on Osteoporosis Prevention, Diagnosis, and Therapy. Osteoporosis prevention, diagnosis, and therapy. *JAMA* 2001 **285** 785–795. (https://doi.org/10.1001/jama.285.6.785)

2 Jain RK & Vokes T. Dual-energy X-ray absorptiometry. *Journal of Clinical Densitometry* 2017 **20** 291–303. (https://doi.org/10.1016/j.jocd.2017.06.014)

3 Wong SC, Khanna S, Rashid R & Ahmed SF. Auditing bone densitometry and fractures in children with chronic disease. *Archives of Disease in Childhood* 2008 **93** 705–707. (https://doi.org/10.1136/adc.2007.118265)

4 Ahmed SF & Elmantaser M. Secondary osteoporosis. *Endocrine Development* 2009 **16** 170–190. (https://doi.org/10.1159/000223695)

5 Hu L, Yin C, Zhao F, Ali A, Ma J & Qian A. Mesenchymal stem cells: cell fate decision to osteoblast or adipocyte and application in osteoporosis treatment. *International Journal of Molecular Sciences* 2018 **19** 360. (https://doi.org/10.3390/ijms19020360)

6 Paccou J, Penel G, Chauveau C, Cortet B & Hardouin P. Marrow adiposity and bone: review of clinical implications. *Bone* 2019 **118** 8–15. (https://doi.org/10.1016/j.bone.2018.02.008)

7 Joseph S, McCarrison S & Wong SC. Skeletal fragility in children with chronic disease. *Hormone Research in Paediatrics* 2016 **86** 71–82. (https://doi.org/10.1159/000447583)

8 Chang G, Boone S, Martel D, Rajapakse CS, Hallyburton RS, Valko M, Honig S & Regatte RR. MRI assessment of bone structure and microarchitecture. *Journal of Magnetic Resonance Imaging* 2017 **46** 323–337. (https://doi.org/10.1002/jmri.25647)

9 Ladinsky GA, Vasilic B, Popescu AM, Wald M, Zemel BS, Snyder PJ, Loh L, Song HK, Saha PK, Wright AC, *et al.* Trabecular structure quantified with the MRI-based virtual bone biopsy in postmenopausal women contributes to vertebral deformity burden independent of areal vertebral BMD. *Journal of Bone and Mineral Research* 2008 **23** 64–74. (https://doi.org/10.1359/jbmr.070815)

10 Mitra S, Fernandez-Del-Valle M & Hill JE. The role of MRI in understanding the underlying mechanisms in obesity associated diseases. *Biochimica et Biophysica Acta: Molecular Basis of Disease* 2017 **1863** 1115–1131. (https://doi.org/10.1016/j.bbadis.2016.09.008)

11 Majumdar S, Newitt D, Mathur A, Osman D, Gies A, Chiu E, Lotz J, Kinney J & Genant H. Magnetic resonance imaging of trabecular bone structure in the distal radius: relationship with X-ray tomographic microscopy and biomechanics. *Osteoporosis International* 1996 **6** 376–385. (https://doi.org/10.1007/BF01623011)

12 Schellinger D, Lin CS, Hatipoglu HG & Fertikh D. Potential value of vertebral proton MR spectroscopy in determining bone weakness. *American Journal of Neuroradiology* 2001 **22** 1620–1627.

13 McComb C, Harpur A, Yacoubian C, Leddy C, Anderson G, Shepherd S, Perry C, Shaikh MG, Foster J & Ahmed SF. MRI-based abnormalities in young adults at risk of adverse bone health due to childhood-onset metabolic and endocrine conditions. *Clinical Endocrinology* 2014 **80** 811–817. (https://doi.org/10.1111/cen.12367)

14 Mostoufi-Moab S, Magland J, Isaacoff EJ, Sun W, Rajapakse CS, Zemel B, Wehrli F, Shekdar K, Baker J, Long J, *et al.* Adverse fat depots and marrow adiposity are associated with skeletal deficits and insulin resistance in long-term survivors of pediatric hematopoietic stem cell transplantation. *Journal of Bone and Mineral Research* 2015 **30** 1657–1666. (https://doi.org/10.1002/jbmr.2512)

15 Modlesky CM, Bajaj D, Kirby JT, Mulrooney BM, Rowe DA & Miller F. Sex differences in trabecular bone microarchitecture are not detected in pre and early pubertal children using magnetic resonance imaging. *Bone* 2011 **49** 1067–1072. (https://doi.org/10.1016/j.bone.2011.07.041)

16 Ruschke S, Pokorney A, Baum T, Eggers H, Miller JH, Hu HH & Karampinos DC. Measurement of vertebral bone marrow proton density fat fraction in children using quantitative water–fat MRI. *Magma* 2017 **30** 449–460. (https://doi.org/10.1007/s10334-017-0617-0)

17 Kugel H, Jung C, Schulte O & Heindel W. Age- and sex-specific differences in the 1H-spectrum of vertebral bone marrow. *Journal of Magnetic Resonance Imaging* 2001 **13** 263–268. (https://doi.org/10.1002/1522-2586(200102)13:2<263::aid-jmri1038>3.0.co;2-m)

18 Roldan-Valadez E, Piña-Jimenez C, Favila R & Rios C. Gender and age groups interactions in quantifying bone marrow fat content in lumbar spine using 3T MR spectroscopy: a multivariate analysis of covariance (mancova). *European Journal of Radiology* 2013 **82** 697–702. (https://doi.org/10.1016/j.ejrad.2013.07.012)

19 Gao Y, Zong K, Gao Z, Rubin MR, Chen J, Heymsfield SB, Gallagher D & Shen W. Magnetic resonance imaging–measured bone marrow adipose tissue area is inversely related to cortical bone area in children and adolescents aged 5–18 years. *Journal of Clinical Densitometry* 2015 **18** 203–208. (https://doi.org/10.1016/j.jocd.2015.03.002)

20 Burkhardt R, Kettner G, Bohm W, Schmidmeier M, Schlag R, Frisch B, Mallmann B, Eisenmenger W & Gilg T. Changes in trabecular bone, hematopoiesis and bone marrow vessels in aplastic anemia, primary osteoporosis, and old age: a comparative histomorphometric study. *Bone* 1987 **8** 157–164. (https://doi.org/10.1016/8756-3282(87)90015-9)

21 Steell L, Johnston BA, Dewantoro D, Foster JE, Gaya DR, Macdonald J, McMillan M, Russell RK, Seenan JP, Ahmed SF, *et al.* Muscle deficits with normal bone microarchitecture and geometry in young adults with well-controlled childhood-onset Crohn's disease. *European Journal of Gastroenterology and Hepatology* 2020 **32** 1497–1506. (https://doi.org/10.1097/MEG.0000000000001838)

22 Morrow JM, Sinclair CD, Fischmann A, Machado PM, Reilly MM, Yousry TA, Thornton JS & Hanna MG. MRI biomarker assessment of neuromuscular disease progression: a prospective observational cohort study. *Lancet: Neurology* 2016 **15** 65–77. (https://doi.org/10.1016/S1474-4422(15)00242-2)

23 Vanhamme L, van den Boogaart A & Van Huffel S. Improved method for accurate and efficient quantification of MRS data with use of prior knowledge. *Journal of Magnetic Resonance* 1997 **129** 35–43. (https://doi.org/10.1006/jmre.1997.1244)

24 Naressi A, Couturier C, Devos JM, Janssen M, Mangeat C, De Beer R & Graveron-Demilly D. Java-based graphical user interface for the MRUI quantitation package. *Magma* 2001 **12** 141–152. (https://doi.org/10.1007/BF02668096)

25 Schellinger D, Lin CS, Lim J, Hatipoglu HG, Pezzullo JC & Singer AJ. Bone marrow fat and bone mineral density on proton MR spectroscopy and dual-energy X-ray absorptiometry: their ratio as a new indicator of bone weakening. *American Journal of Roentgenology* 2004 **183** 1761–1765. (https://doi.org/10.2214/ajr.183.6.01831761)

26 Khosla S, Melton LJ, Robb RA, Camp JJ, Atkinson EJ, Oberg AL, Rouleau PA & Riggs BL. Relationship of volumetric BMD and structural parameters at different skeletal sites to sex steroid levels in men. *Journal of Bone and Mineral Research* 2005 **20** 730–740. (https://doi.org/10.1359/JBMR.041228)

27 Riggs BL, Melton III LJ, Robb RA, Camp JJ, Atkinson EJ, McDaniel L, Amin S, Rouleau PA & Khosla S. A population-based assessment of rates of bone loss at multiple skeletal sites: evidence for substantial trabecular bone loss in young adult women and men. *Journal of Bone and Mineral Research* 2008 **23** 205–214. (https://doi.org/10.1359/jbmr.071020)

28 Majumdar S, Kothari M, Augat P, Newitt DC, Link TM, Lin JC, Lang T, Lu Y & Genant HK. High-resolution magnetic resonance imaging: three-dimensional trabecular bone architecture and biomechanical properties. *Bone* 1998 **22** 445–454. (https://doi.org/10.1016/s8756-3282(98)00030-1)

29 Link TM, Majumdar S, Lin JC, Newitt D, Augat P, Ouyang X, Mathur A & Genant HK. A comparative study of trabecular bone properties in the spine and femur using high resolution MRI and CT. *Journal of Bone and Mineral Research* 1998 **13** 122–132. (https://doi.org/10.1359/jbmr.1998.13.1.122)

30 Gosman JH & Ketcham RA. Patterns in ontogeny of human trabecular bone from SunWatch Village in the Prehistoric Ohio Valley: general features of microarchitectural change. *American Journal of Physical Anthropology* 2009 **138** 318–332. (https://doi.org/10.1002/ajpa.20931)

31 Ortoft G, Andreassen TT & Oxlund H. The influence of growth hormone on cancellous and cortical bone of the vertebral body in aged rats. *Journal of Bone and Mineral Research* 1996 **11** 1094–1102. (https://doi.org/10.1002/jbmr.5650110808)

32 Ohlsson C, Bengtsson BA, Isaksson OG, Andreassen TT & Slootweg MC. Growth hormone and bone. *Endocrine Reviews* 1998 **19** 55–79. (https://doi.org/10.1210/edrv.19.1.0324)

33 Venken K, De Gendt K, Boonen S, Ophoff J, Bouillon R, Swinnen JV, Verhoeven G & Vanderschueren D. Relative impact of androgen and estrogen receptor activation in the effects of androgens on trabecular and cortical bone in growing male mice: a study in the androgen receptor knockout mouse model. *Journal of Bone and Mineral Research* 2006 **21** 576–585. (https://doi.org/10.1359/jbmr.060103)

34 Nishiyama KK, Macdonald HM, Moore SA, Fung T, Boyd SK & McKay HA. Cortical porosity is higher in boys compared with girls at the distal radius and distal tibia during pubertal growth: an HR-pQCT study. *Journal of Bone and Mineral Research* 2012 **27** 273–282. (https://doi.org/10.1002/jbmr.552)

35 Kirmani S, Christen D, van Lenthe GH, Fischer PR, Bouxsein ML, McCready LK, Melton LJ, 3rd, Riggs BL, Amin S, Muller R, *et al.* Bone structure at the distal radius during adolescent growth. *Journal of Bone and Mineral Research* 2009 **24** 1033–1042. (https://doi.org/10.1359/jbmr.081255)

36 Glorieux FH, Travers R, Taylor A, Bowen JR, Rauch F, Norman M & Parfitt AM. Normative data for iliac bone histomorphometry in growing children. *Bone* 2000 **26** 103–109. (https://doi.org/10.1016/s8756-3282(99)00257-4)

37 Griffin LM, Honig S, Chen C, Saha PK, Regatte R & Chang G. 7T MRI of distal radius trabecular bone microarchitecture: how trabecular bone quality varies depending on distance from end-of-bone. *Journal of Magnetic Resonance Imaging* 2017 **45** 872–878. (https://doi.org/10.1002/jmri.25398)

38 Seeman E & Ghasem-Zadeh A. Challenges in the acquisition and analysis of bone microstructure during growth. *Journal of Bone and Mineral Research* 2016 **31** 2239–2241. (https://doi.org/10.1002/jbmr.3015)

39 Karampinos DC, Ruschke S, Gordijenko O, Grande Garcia E, Kooijman H, Burgkart R, Rummeny EJ, Bauer JS & Baum T. Association of MRS-based vertebral bone marrow fat fraction with bone strength in a human in vitro model. *Journal of Osteoporosis* 2015 **2015** 152349. (https://doi.org/10.1155/2015/152349)

40 Cohen A, Dempster DW, Stein EM, Nickolas TL, Zhou H, McMahon DJ, Muller R, Kohler T, Zwahlen A, Lappe JM, *et al.* Increased marrow adiposity in premenopausal women with idiopathic osteoporosis. *Journal of Clinical Endocrinology and Metabolism* 2012 **97** 2782–2791. (https://doi.org/10.1210/jc.2012-1477)

41 Li X, Cui Q, Kao C, Wang GJ & Balian G. Lovastatin inhibits adipogenic and stimulates osteogenic differentiation by suppressing PPARgamma2 and increasing Cbfa1/Runx2 expression in bone marrow mesenchymal cell cultures. *Bone* 2003 **33** 652–659. (https://doi.org/10.1016/s8756-3282(03)00239-4)

42 Wang Q, Wang XF, Iuliano-Burns S, Ghasem-Zadeh A, Zebaze R & Seeman E. Rapid growth produces transient cortical weakness: a risk factor for metaphyseal fractures during puberty. *Journal of Bone and Mineral Research* 2010 **25** 1521–1526. (https://doi.org/10.1002/jbmr.46)

43 Gilsanz V, Skaggs DL, Kovanlikaya A, Sayre J, Loro ML, Kaufman F & Korenman SG. Differential effect of race on the axial and appendicular skeletons of children. *Journal of Clinical Endocrinology and Metabolism* 1998 **83** 1420–1427. (https://doi.org/10.1210/jcem.83.5.4765)

44 Loro ML, Sayre J, Roe TF, Goran MI, Kaufman FR & Gilsanz V. Early identification of children predisposed to low peak bone mass and osteoporosis later in life. *Journal of Clinical Endocrinology and Metabolism* 2000 **85** 3908–3918. (https://doi.org/10.1210/jcem.85.10.6887)

45 Högler W, Blimkie CJ, Cowell CT, Kemp AF, Briody J, Wiebe P, Farpour-Lambert N, Duncan CS & Woodhead HJ. A comparison of bone geometry and cortical density at the mid-femur between prepuberty and young adulthood using magnetic resonance imaging. *Bone* 2003 **33** 771–778. (https://doi.org/10.1016/s8756-3282(03)00266-7)

46 van der Meulen MC, Ashford Jr MW, Kiratli BJ, Bachrach LK & Carter DR. Determinants of femoral geometry and structure during adolescent growth. *Journal of Orthopaedic Research* 1996 **14** 22–29. (https://doi.org/10.1002/jor.1100140106)

47 Rauch F, Klein K, Allolio B & Schonau E. Age at menarche and cortical bone geometry in premenopausal women. *Bone* 1999 **25** 69–73. (https://doi.org/10.1016/s8756-3282(99)00104-0)

48 Witzke KA & Snow CM. Lean body mass and leg power best predict bone mineral density in adolescent girls. *Medicine and Science in Sports and Exercise* 1999 **31** 1558–1563. (https://doi.org/10.1097/00005768-199911000-00010)

49 Schwartz AV, Sigurdsson S, Hue TF, Lang TF, Harris TB, Rosen CJ, Vittinghoff E, Siggeirsdottir K, Sigurdsson G, Oskarsdottir D, *et al.* Vertebral bone marrow fat associated with lower trabecular BMD and prevalent vertebral fracture in older adults. *Journal of Clinical Endocrinology and Metabolism* 2013 **98** 2294–2300. (https://doi.org/10.1210/jc.2012-3949)

50 Justesen J, Stenderup K, Ebbesen EN, Mosekilde L, Steiniche T & Kassem M. Adipocyte tissue volume in bone marrow is increased with aging and in patients with osteoporosis. *Biogerontology* 2001 **2** 165–171. (https://doi.org/10.1023/a:1011513223894)

51 Griffith JF, Yeung DK, Ma HT, Leung JCS, Kwok TC & Leung PC. Bone marrow fat content in the elderly: a reversal of sex difference seen in younger subjects. *Journal of Magnetic Resonance Imaging* 2012 **36** 225–230. (https://doi.org/10.1002/jmri.23619)

52 Baum T, Rohrmeier A, Syväri J, Diefenbach MN, Franz D, Dieckmeyer M, Scharr A, Hauner H, Ruschke S, Kirschke JS, *et al.* Anatomical variation of age-related changes in vertebral bone marrow composition using chemical shift encoding-based water–fat magnetic resonance imaging. *Frontiers in Endocrinology* 2018 **9** 141. (https://doi.org/10.3389/fendo.2018.00141)

53 Singhal V, Karzar NH, Bose A, Buckless C, Ackerman KE, Bredella MA, Klibanski A & Misra M. Changes in marrow adipose tissue in relation to changes in bone parameters following estradiol replacement in adolescent and young adult females with functional hypothalamic amenorrhea. *Bone* 2021 **145** 115841. (https://doi.org/10.1016/j.bone.2021.115841)

54 Abdalrahaman N, McComb C, Foster JE, Lindsay RS, Drummond R, McKay GA, Perry CG & Ahmed SF. The relationship between adiposity, bone density and microarchitecture is maintained in young women irrespective of diabetes status. *Clinical Endocrinology* 2017 **87** 327–335. (https://doi.org/10.1111/cen.13410)

55 Wokke BH, van den Bergen JC, Versluis MJ, Niks EH, Milles J, Webb AG, van Zwet EW, Aartsma-Rus A, Verschuuren JJ & Kan HE. Quantitative MRI and strength measurements in the assessment of muscle quality in duchenne muscular dystrophy. *Neuromuscular Disorders* 2014 **24** 409–416. (https://doi.org/10.1016/j.nmd.2014.01.015)

56 Goodpaster BH, Chomentowski P, Ward BK, Rossi A, Glynn NW, Delmonico MJ, Kritchevsky SB, Pahor M & Newman AB. Effects of physical activity on strength and skeletal muscle fat infiltration in older adults: a randomized controlled trial. *Journal of Applied Physiology* 2008 **105** 1498–1503. (https://doi.org/10.1152/japplphysiol.90425.2008)

57 Kirkland JL, Tchkonia T, Pirtskhalava T, Han J & Karagiannides I. Adipogenesis and aging: does aging make fat go MAD? *Experimental Gerontology* 2002 **37** 757–767. (https://doi.org/10.1016/s0531-5565(02)00014-1)

58 Gallagher D, Kuznia P, Heshka S, Albu J, Heymsfield SB, Goodpaster B, Visser M & Harris TB. Adipose tissue in muscle: a novel depot similar in size to visceral adipose tissue. *American Journal of Clinical Nutrition* 2005 **81** 903–910. (https://doi.org/10.1093/ajcn/81.4.903)

59 Delmonico MJ, Harris TB, Visser M, Park SW, Conroy MB, Velasquez-Mieyer P, Boudreau R, Manini TM, Nevitt M, Newman AB, *et al.* Longitudinal study of muscle strength, quality, and adipose tissue infiltration. *American Journal of Clinical Nutrition* 2009 **90** 1579–1585. (https://doi.org/10.3945/ajcn.2009.28047)

60 Yim JE, Heshka S, Albu JB, Heymsfield S & Gallagher D. Femoral-gluteal subcutaneous and intermuscular adipose tissues have independent and opposing relationships with CVD risk. *Journal of Applied Physiology* 2008 **104** 700–707. (https://doi.org/10.1152/japplphysiol.01035.2007)

61 Triplett WT, Baligand C, Forbes SC, Willcocks RJ, Lott DJ, DeVos S, Pollaro J, Rooney WD, Sweeney HL, Bönnemann CG, *et al.* Chemical shift-based MRI to measure fat fractions in dystrophic skeletal muscle. *Magnetic Resonance in Medicine* 2014 **72** 8–19. (https://doi.org/10.1002/mrm.24917)

Received in final form 21 May 2022
Accepted 13 June 2022
Accepted Manuscript published online 14 June 2022